Spatial properties of coaxial superposition of two coherent Gaussian beams

Boualem Boubaha,[1] Darryl Naidoo,[2] Thomas Godin,[3] Michael Fromager,[4] Andrew Forbes,[2,5] and Kamel Aït-Ameur[4,*]

[1]Faculté de Physique, Université des Sciences et de la Technologie Houari Boumédiène, B.P. n° 32, El Alia, 16111 Algiers, Algeria

[2]Council for Scientific and Industrial Research, National Laser Centre, P.O. Box 395, Pretoria 0001, South Africa

[3]Institut Franche Comté Electronique Mécanique Thermique et Optique-Sciences et Technologies, Centre National de la Recherche Scientifique—Université de Franche-Comté, Unité Mixte de Recherche 6174, 25030 Besançon, France

[4]Centre de Recherche sur les Ions, les Matériaux et la Photonique, Unité Mixte de Recherche de Recherche 6252, Commissariat à l'Energie Atomique, Centre National de la Recherche Scientifique, Université de Caen Basse Normandie, Ecole Nationale Supérieure des Ingénieurs de Caen, Boulevard Maréchal Juin, F14050 Caen, France

[5]School of Physics, University of KwaZulu-Natal, Private Bag X54001, Durban 4000, South Africa

*Corresponding author: kamel.aitameur@ensicaen.fr

Received 28 May 2013; revised 18 July 2013; accepted 18 July 2013; posted 19 July 2013 (Doc. ID 191202); published 7 August 2013

In this paper, we explore theoretically and experimentally the laser beam shaping ability resulting from the coaxial superposition of two coherent Gaussian beams (GBs). This technique is classified under interferometric laser beam shaping techniques contrasting with the usual ones based on diffraction. The experimental setup does not involve the use of some two-wave interferometer but uses a spatial light modulator for the generation of the necessary interference term. This allows one to avoid the thermal drift occurring in interferometers and gives a total flexibility of the key parameter setting the beam transformation. In particular, we demonstrate the reshaping of a GB into a bottle beam or top-hat beam in the focal plane of a focusing lens. © 2013 Optical Society of America

OCIS codes: (140.3300) Laser beam shaping; (140.3298) Laser beam combining.
http://dx.doi.org/10.1364/AO.52.005766

1. Introduction

Many commercial laser systems deliver a beam having a Gaussian intensity profile; however, numerous applications require other intensity profiles (top-hat, hollow beam, Bessel beam) that are in general obtained by converting the standard Gaussian beam (GB) through transparent diffractive optical elements (DOEs). Laser beam shaping by use of DOEs is a topic that has been intensively developed over a long time [1,2] whether the DOE is programmable or unprogrammable. The first kind of programmable DOE is based on liquid crystal optical valves or deformable mirrors, which have the advantage of being very flexible. Unprogrammable DOEs consist of a transparent material in which an adequate relief is etched giving rise to a desired phase shift profile where the relief can be continuous or discrete (32 or 64 phase levels). Our objective in this

1559-128X/13/235766-07$15.00/0

paper is to study a supplementary technique of laser beam shaping based on the coaxial superposition of two coherent GBs. This technique is classified under interferometric laser beam shaping, which contrasts with the usual one based on diffraction. Interesting features from laser beam shaping using interferometric techniques have been already demonstrated in literature. For instance, the generation of a focal spot having a size smaller than that of a GB has been proven from the axial superposition of two GBs that were orthogonally polarized with their beam waist planes shifted. Since the Gouy phase difference associated with the two beams exits only in the vicinity of the focal plane, it results in a polarization component having the property of superresolution which improves the longitudinal and transversal resolutions with a rate of about 30% [3]. Another example of interferometric beam shaping consists of generating optical vortices [4–6].

The main contributions in the area of laser beam shaping based on interferometric techniques are devoted to the generation of optical bottle beams (OBBs). This is a concept of a beam that is characterized by a dark (minimal intensity) region that is surrounded by higher intensity light in the three principal directions. The OBB is very useful for trapping particles having a refractive index lower than the surrounding medium [7]. Before proceeding, we consider some experiments described in literature for generating such OBBs:

(i) An OBB has been generated from the interference between Laguerre–Gauss beams LG_{00} and LG_{20}. The latter is obtained from a LG_{00} beam that is transformed into a LG_{20} by the use of a computer-generated hologram [8] external to a laser cavity that supplied the LG_{00} beam. It has been found that the optical barrier along the beam axis is roughly 3 times higher in the radial direction.

(ii) Another solution is to generate directly inside a laser made up of a degenerate resonator the family of transverse modes LG_{p0} with $p = 0, 3, 6, \ldots$ Since all these modes have the same frequency, they can interfere and give rise to a bottle beam near the focus of a converging lens [9,10].

(iii) In [11], the OBB results from the interference of two Bessel beams that are generated by using a spatial light modulator (SLM).

(iv) In [12], the OBB is obtained by the destructive interference of two GBs with different waists but focused in the same plane where the reshaping is achieved. The two GBs emerge from a Mach–Zehnder interferometer with a feedback circuit for locking the two beams out of phase through the action of a piezoelectric mirror mounted in one arm.

In this paper, we will consider the spatial properties of the coaxial superposition of two coherent GBs having the same width but opposite curvature in the plane of a focusing lens. In this case the two GBs will focus in different planes. This is very different from the case addressed in [12] which considers the focusing of two GBs of different widths, same curvatures, and focusing in the same plane. In particular, in addition to the usual bottle beam we demonstrate theoretically and experimentally that it is possible to reshape a GB into a top-hat profile in the focal plane of a lens.

2. Coaxial Superposition of Two Coherent Gaussian Beams

Essentially, the coaxial superposition of two coherent GBs gives rise to a beam that is made up of a certain adjustable number of rings of light, which is in the following termed a cosine Gaussian beam (CGB).

The CGB we wish to generate is described by the following electric field:

$$u(r) = E_0 \cos(\beta r^2) \exp\left[-\frac{r^2}{W^2}\right], \tag{1}$$

where β is effectively a quantity inversely proportional to a squared length. Through analogy with the argument of the Gaussian term in Eq. (1) we arbitrarily set the following expression for β:

$$\beta = \frac{2\pi K}{W^2}, \tag{2}$$

where W is the GB width and the number K is real and constitutes the key parameter of the interferometric beam shaping as it will be seen in the following. Figure 1 illustrates the intensity distribution of a CGB, $I(r) = |u(r)|^2$, for $K = 2$ and $W = 1$ mm.

The ringed beam described by Eq. (1) contains a modulating term $\cos(\beta r^2)$ having its origin, not in a planar phase difference between the two GBs, but in the interference between two spherical wavefronts with opposite radii of curvature as it will be shown below. The CGB described by Eq. (1) can be viewed as the coaxial superposition of two GBs having the same width W and opposite radii of curvature (R):

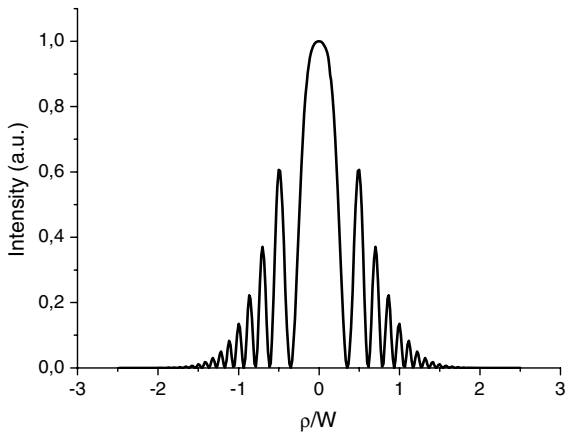

Fig. 1. Transverse intensity distribution $I(\rho) = |u(\rho)|^2$ of the CGB $u(\rho)$ defined by Eqs. (1) and (2) for $K = 2$ and $W = 1$ mm.

$$u(r) = \frac{E_0}{2}\left\{\exp\left[-\frac{ikr^2}{2R}\right]\exp\left[-\frac{r^2}{W^2}\right] + \exp\left[+\frac{ikr^2}{2R}\right]\exp\left[-\frac{r^2}{W^2}\right]\right\}. \quad (3)$$

In these conditions Eq. (3) takes the form of Eq. (1) provided we set

$$\frac{K}{W^2} = \frac{1}{2\lambda R}. \quad (4)$$

In the following, we will be interested in the focusing of the CGB by a converging lens. The determination of the field emerging from the lens can be very simple if the field $u(r)$ is formulated by Eq. (3) or more complicated when using Eq. (1). Indeed, the later case necessitates the numerical calculation of a Fresnel–Kirchhoff integral, while the use of Eq. (3) allows one to obtain after the lens, the emerging field from the complex addition of two GBs. In addition, considering Eq. (3) makes the interpretation of the results tremendously easier.

There are two cases that occur simultaneously to the field u given by Eq. (3) when passed through a focusing lens of focal length f. Beginning at the exit plane of the lens, the first case is that one of the GBs will *always* focus at some position along the propagation axis. The second case concerns the second GB and is comprised of three scenarios, as is illustrated in Fig. 2:

(i) Scenario No. 1: The beam will also focus at some position along the propagation axis, typically after the focus of the first GB.
(ii) Scenario No. 2: The beam will be collimated during propagation.
(iii) Scenario No. 3: The beam will diverge during propagation with a virtual focal point positioned before the entrance of the lens.

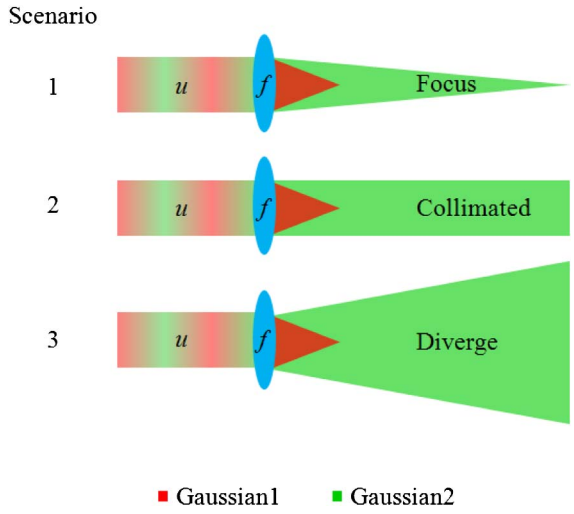

Fig. 2. Three possible scenarios for the behavior of the two GBs superimposed in the field u.

It must be noted that for scenario No. 1, the second focus will always be larger than the first. Scenario No. 2 is achieved by equating the curvature of the field to the focal length of the lens, $R = f$ and from Eq. (4), we find that this condition equates to

$$K_c = \frac{W^2}{2\lambda R}. \quad (5)$$

This particular value of K given by Eq. (5) is considered to be the critical value where scenario No. 1 is achieved for values of K less than K_c, and scenario No. 3 is achieved for values of K larger than K_c. In a more practical formulation, this can be summarized as follows:

– For $R > f$, one observes two focal points.
– For $R \le f$, one observes only one focal point.

Let us consider two GBs having the same width W and radii of curvature $R_1 = R$ and $R_2 = -R$ incident on a focusing lens of focal length f. After the lens, the radius of curvature becomes

$$R'_{1,2} = \frac{fR_{1,2}}{f - R_{1,2}} \quad (6)$$

and the beam waist radius W'_{01} and W'_{02} associated with the transformed beams are given by

$$W'_{01,2} = \frac{W}{\sqrt{1 + \left(\frac{\pi W^2}{\lambda R'_{1,2}}\right)^2}}. \quad (7)$$

The locations Z'_{01} and Z'_{02} of the beam waist planes are different and given by

$$Z'_{01,2} = \frac{R'_{1,2}}{1 + \left(\frac{\lambda R'_{1,2}}{\pi W^2}\right)^2}. \quad (8)$$

The beam waist position of the transformed GB is beyond (respectively, before the lens) the lens if the radius of curvature R' given by Eq. (6) is negative (respectively, positive).

In the following we will determine the electrical field after the lens at the position Z, which is written $Z'_{1,2} = Z + Z'_{01,2}$ with respect to the beam-waist positions Z'_{01} and Z'_{02} of the transformed beams. The expression of the electrical field u'_1 and u'_2 associated with the two transformed GBs at position Z after the lens is given by

$$u'_{1,2} = E'_{01,2} \cdot \frac{W'_{01,2}}{W'_{1,2}} \exp\left[-\frac{r^2}{W'^2_{1,2}}\right] \times \exp\left[-i\left(kZ'_{1,2} + \frac{kr^2}{2R'_{1,2}} - \mathrm{arctg}\left(\frac{Z'_{1,2}}{Z'_{R1,2}}\right)\right)\right], \quad (9)$$

where

$$Z'_{R1,2} = \frac{\pi W'^2_{01,2}}{\lambda} \quad \text{and} \quad W'_{1,2} = W'_{01,2}\sqrt{1+\left(\frac{Z'_{1,2}}{Z'_{R1,2}}\right)^2}$$

$$\text{and} \quad R'_{1,2} = Z'_{1,2}\left[1+\left(\frac{Z'_{R1,2}}{Z'_{1,2}}\right)^2\right]. \tag{10}$$

The electric field anywhere after the lens is given by $u' = u'_1 + u'_2$, and the intensity is expressed as $I = |u'|^2$. Before proceeding, we express the amplitude E'_{01} and E'_{02} [in Eq. (9)] of the transformed beams as a function of $E_0/2$ [Eq. (3)], the amplitude of the two incident GBs on the lens. By equalizing the amplitude E'_{01} and E'_{02} with $E_0/2$ at the center of the lens ($r = 0$), we find

$$E'_{02} = E'_{01} \cdot \frac{W'_{01}}{W'_{02}}. \tag{11}$$

In order to characterize the beam, after the lens, resulting from the coaxial superposition of two coherent GBs, we will consider the variations of the on-axis intensity (i.e., for $r = 0$) and the radial intensity distributions. The numerical calculations are performed for $K = 3, f = 200$ mm, $W = 2.5$ mm, and $\lambda = 1064$ nm. The on-axis intensity distribution plotted in Fig. 3 shows as expected two focal points located before ($Z = 166$ mm) and beyond ($Z = 250$ mm) the focal plane of the lens ($Z = 200$ mm) with their respective transverse intensity profiles in Figs. 4(a) and 4(b). The pattern in the focal plane of the lens is displayed in Fig. 4(c) and exhibits a ringed beam (14 rings) with a central null-intensity region. One observes that the intensity of the second focal point is smaller than that of the first focal point owing to its larger diameter, and subsequently decreases as K increases.

3. Interferometric Beam Shaping

An interesting feature of the CGB is when the parameter K is reduced, one observes that the number of rings shown in Fig. 1 reduces while the on-axis intensity peaks shown in Fig. 3 get closer until overlapping. In the following, it will be shown that the CGB described by Eq. (1) allows the possibility of generating:

– a flat-top intensity pattern
– an OBB, that is a three-dimensional region in which the intensity is low and surrounded by regions of higher intensity.

Let us now consider the requirements for converting the incident GB into a flat-top distribution at the focal plane $z = f$. The results are presented

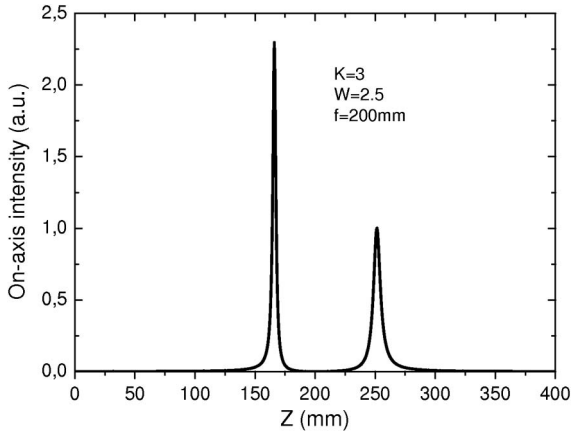

Fig. 3. On-axis intensity distribution of the focused mixed two GBs for $K = 3$ and $W = 2.5$ mm. The focusing lens has a focal length $f = 200$ mm. As parameter K is reduced, one observes that the two intensity peaks get closer until overlapping.

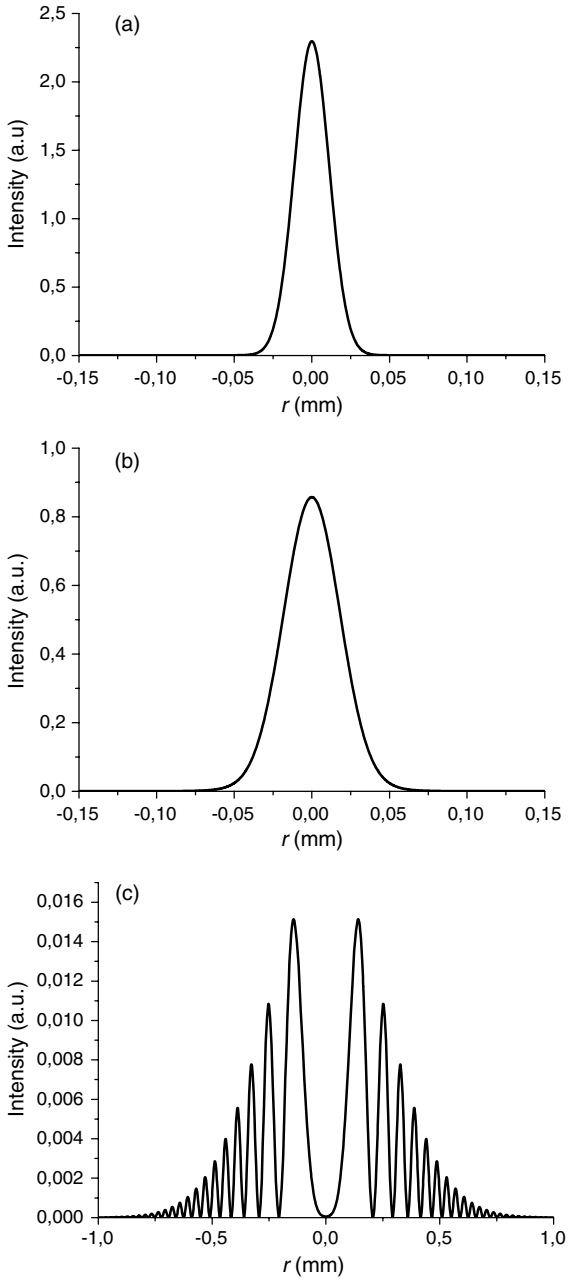

Fig. 4. Transverse intensity distribution, for $K = 3$ and $W = 2.5$ mm, in three planes: (a) $Z = 166$ mm, i.e., the first focusing plane in Fig. 4, (b) $Z = 250$ mm, i.e., the second focusing plane in Fig. 4, and (c) $Z = f = 200$ mm, i.e., the focal plane of the lens.

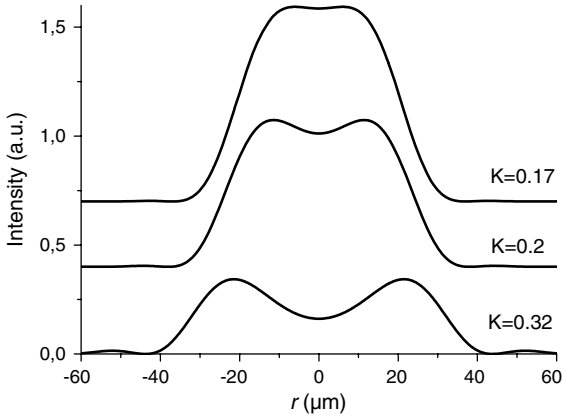

Fig. 5. Transverse intensity distribution, for $W = 2.5$ mm, in the focal plane of the focusing lens of focal length $f = 125$ mm. For $K = 0.17$, the incident GB is transformed into a top-hat profile.

in Fig. 5 where the focal plane intensity distributions are plotted for several values of parameter K. It is seen that the intensity distribution changes as parameter K is varied: for K close to zero (not shown) it is a Gaussian profile, developing into a close replica of the top-hat profile for $K = 0.17$, then acquiring a doughnut profile for $K = 0.32$, hence becoming a hollow beam, as shown in Fig. 4(c) for higher values for K. It is remarkable to notice that the beam shaping properties displayed in Fig. 5 are obtained from the interference of two coherent GBs, which are coaxially superposed by resorting to a two-wave interferometer or by generating the modulating term $\cos(\beta r^2)$ with a SLM. In the experiment, as it will be shown below, we have preferred to make the coaxial superposition of two GBs by using the SLM solution. Doing so allows some flexibility in the beam shaping since the reshaped beam pattern can continuously evolve by adjusting the parameter K. It also results that the two GBs involved in Eq. (9) have the same phase on the focusing lens. For doing so, a phase shift $\Delta\varphi$ ranging from 0 to 2π is added, so that u_1' and u_2' should be in phase, for instance at the center of the lens ($r = 0$). In addition, the SLM solution for generating the CGB described by Eq. (1) allows one to avoid the phase shift drift due to vibrations and thermal effects, which is an inherent limitation of interferometric devices.

We have found that we are able to produce a bottle beam from the coaxial superposition of two coherent GBs straddling the focal plane of a converging lens. The result is shown in Fig. 6 for $K = 0.4$, and we can note that the quality of the OBB is highly satisfying. Indeed, the optical barrier along the beam axis is about 3.5 times higher than that in the radial direction, and this result is comparable to what is reported in [8]. It is worthwhile to note that the size of the bottle beam as well as the two surrounding focal spots can be adjusted by varying the parameter K. This is easily achievable with a SLM, thus making the setup very versatile.

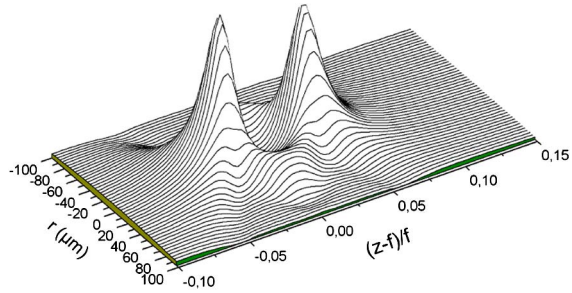

Fig. 6. For $K = 0.4$ the coaxial superposition of two coherent GBs is able to produce a bottle beam straddling the focal plane $Z = f$ of the focusing lens.

4. Experimental Investigation

As pointed out in Section 3 we experimentally generate the CGB expressed by Eq. (1) by generating the $\cos(\beta r^2)$ term by using a SLM. This has two advantages:

(i) We avoid all the drawbacks to the phase shift drift inherent to any interferometer due to thermal effects and vibrations.
(ii) The flexibility linked to the possible continuous adjustment of parameter K.

The experimental setup (Fig. 7) consisted of a laser source operating at 1064 nm with a Gaussian intensity profile as the output. This beam was enlarged and collimated through a 20× telescope and propagated onto a reflective phase-only liquid crystal on silicon (SLM: Holoeye Pluto-NIR). The enlarging and collimating of the laser beam is approximated as a plane wave on the SLM since the active area on the SLM is small as compared to the incident beam size (≈20 mm). The plane of the SLM was imaged through a $4f$ system where the higher orders were spatially filtered at the Fourier plane of the SLM. The beam profile was then monitored along the propagation axis with a CCD camera (Thorlabs cam BC 106-vis).

The incident laser beam on the SLM is required to be a plane wave since we intended to implement the transmission function $\cos(\beta R^2)$, Gaussian field to be

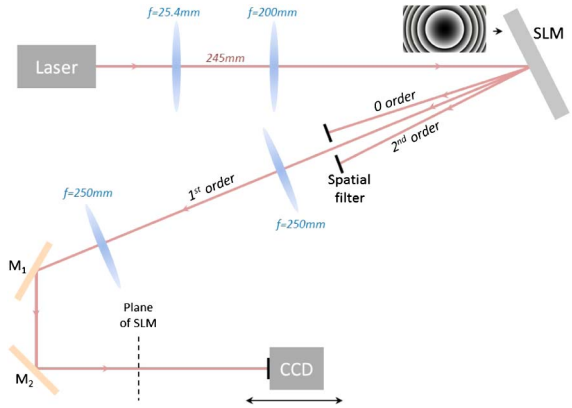

Fig. 7. Experimental setup for investigating the behavior of the superposition of two GBs.

addressed to the SLM. This complete information contains both amplitude and phase and the encoding of the amplitude and phase is through a technique developed in [13,14] to address a phase-only SLM. The complex function $T(r) = A(r)\exp[i\Phi(r)]$ is encoded onto a phase hologram $H(r) = \exp[i\Psi(A,\Phi)]$ with $A \in [0,1]$ and $\Phi \in [-\pi,\pi]$. From the different expressions for $\Psi(A,\Phi)$ used in literature, we have chosen $\Psi(A,\Phi) = f(A)\sin(\Phi)$, where $f(A)$ results from $J_1[f(A)] \approx 0.6A$ with $J_1(x)$ the first-order Bessel function [13]. In addition, the focusing lens f was also encoded onto the hologram with a sinusoidal grating employed as a phase carrier.

This experimental setup was able to exactly reproduce the theoretical results given by Fig. 5, as seen in Fig. 8. The following experimental parameters have been used to encode the hologram: $f = 125$ mm, $W = 0.7$ mm, $z = f$, and $\lambda = 1.064$ μm. The size of the beam has been changed just in order to obtain a sufficiently large picture size on the camera but it did not affect the obtained beam shaping.

The same setup had also confirmed the ability to produce an OBB of good quality. The results are shown in Figs. 9–11, where the behavior of the reshaped beam can be seen from both sides of the focal plane.

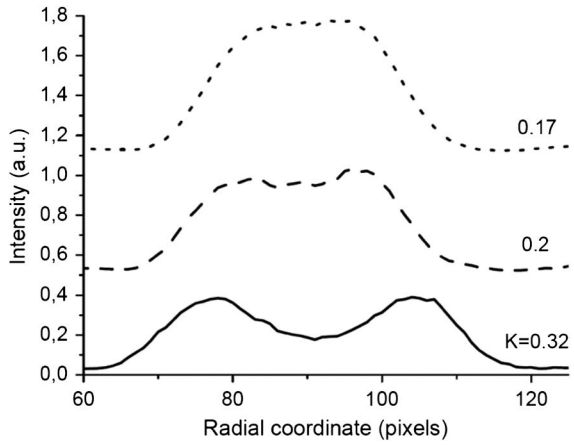

Fig. 8. Experimental beam shaping in the focal plane of the focusing lens with $K = 0.17$, $K = 0.2$, and $K = 0.32$.

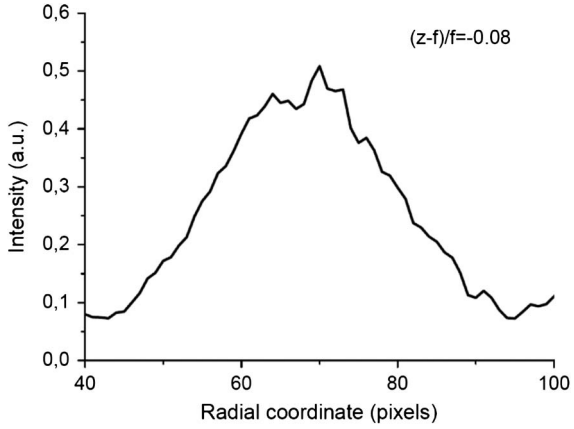

Fig. 9. Experimental beam shaping for $K = 0.4$ before the focal plane, i.e., at $(z-f)/f = -0.08$.

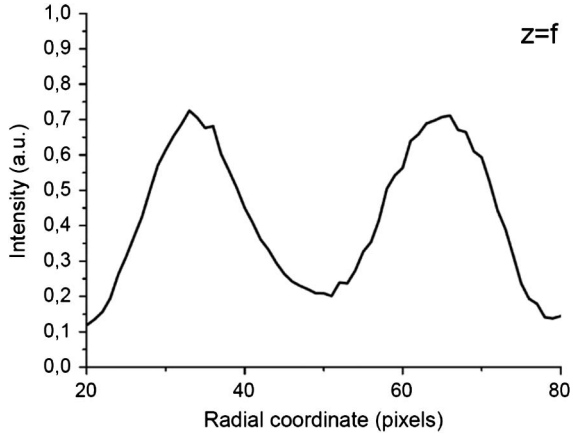

Fig. 10. Experimental beam shaping for $K = 0.4$ at the focal plane, i.e., $z = f$.

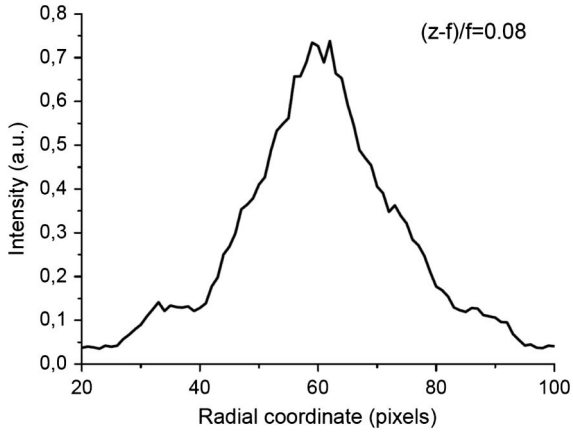

Fig. 11. Experimental beam shaping for $K = 0.4$ after the focal plane, i.e., at $(z-f)/f = +0.08$.

5. Conclusion

In this paper we have analyzed the spatial properties of the beam resulting from the coaxial superposition of two coherent GBs having the same width and opposite radii of curvature. The resulting beam is a CGB expressed by Eq. (1) and we have considered its focusing by a converging lens. Although this technique has to be classified under interferometric laser beam shaping, it has been implemented by a diffractive technique. Indeed, the generation of the $\cos(\beta r^2)$ term defining the CGB has been directly generated by a SLM and in doing so, it has at least two advantages. The first one is that the thermal effects and vibrations do not give rise to phase shift fluctuations which could have a bad influence on the beam shaping stability. The second one is the simplicity and versatility of the setup since the key parameter K (i.e., β) of the beam shaping can be continuously adjusted by the software controlling the SLM. The result should be an intensity distribution in the focal plane of the focusing lens, which could be continuously or abruptly changed from a single-lobed pattern to a

hollow beam. This kind of tailored light distribution could be particularly useful for tweezing and trapping of dielectric micro-sized particles. Indeed, high-index particles can be trapped and manipulated using a trapping beam with a top-hat transverse profile. On the other hand, the annular transverse profile makes it possible to trap high-index particles in the doughnut ring and low-index particles in its dark core.

The authors thank Professor Y. Boudouma from the laboratory SNIM (University of Algiers) for helpful discussions. The authors acknowledge the support of the *Conseil Régional Basse Normandie* (France), the *National Research Foundation* (South Africa), and the *Partenariat Hubert Curien* (France) under the grant PROTEA No. 25886XC. The authors also acknowledge the financial support of the French *Agence Nationale de la Recherche* (ANR), through the program "Investissements d'Avenir" (ANR-10-LABX-09-01), LabEx EMC^3, and the *Fond Européen de Développement Régional*.

References

1. F. M. Dickey and S. G. Holswade, eds., *Laser Beam Shaping* (CRC-Taylor & Francis Group, 2006).
2. V. A. Soifer, ed., *Methods for Computer Design of Diffractive Optical Elements* (Wiley, 2002).
3. J. B. Steward, B. E. A. Saleh, M. C. Teich, and J. T. Fourkas, "Experimental demonstration of polarization-assisted transverse and axial optical superresolution," Opt. Commun. **241**, 315–319 (2004).
4. I. D. Maleev and G. A. Swartzlander, "Composite optical vortices," J. Opt. Soc. Am. B **20**, 1169–1176 (2003).
5. V. Pyragaite and A. Stabinis, "Interference of intersecting singular beams," Opt. Commun. **220**, 247–255 (2003).
6. T. Ando, N. Matsumoto, Y. Ohtake, Y. Takiguchi, and T. Inoue, "Structure of optical singularities in coaxial superpositions of Laguerre–Gaussian modes," J. Opt. Soc. Am. A **27**, 2602–2612 (2010).
7. P. Xu, X. He, J. Wang, and M. Zhan, "Trapping a single atom in a blue detuned optical bottle beam trap," Opt. Lett. **35**, 2164–2166 (2010).
8. J. Arlt and M. J. Padgett, "Generation of a beam with a dark focus surrounded by regions of higher intensity: the optical bottle beam," Opt. Lett. **25**, 191–193 (2000).
9. P. T. Tai, W. F. Hsieh, and C. H. Chen, "Direct generation of optical bottle beams from a tightly focused end-pumped solid-state laser," Opt. Express **12**, 5827–5833 (2004).
10. C. H. Chen, P. T. Tai, and W. F. Hsieh, "Bottle beam from a bare laser for single-beam trapping," Appl. Opt. **43**, 6001–6006 (2004).
11. B. P. S. Ahluwalia, X. C. Yuan, and S. H. Tao, "Generation of self-imaged optical bottle beams," Opt. Commun. **238**, 177–184 (2004).
12. L. Isenhower, W. Williams, A. Dally, and M. Saffman, "Atom trapping in an interferometrically generated bottle beam trap," Opt. Lett. **34**, 1159–1161 (2009).
13. V. Arrizón, U. Ruiz, R. Carrada, and L. A. González, "Pixelated phase computer holograms for the accurate encoding of scalar complex fields." J. Opt. Soc. Am. A **24**, 3500–3507 (2007).
14. D. Flamm, D. Naidoo, C. Schulze, A. Forbes, and M. Duparré, "Mode analysis with a spatial light modulator as a correlation filter," Opt. Lett. **37**, 2478–2480 (2012).